

High Resolution Radar Imaging using Coherent MultiBand Processing Techniques

Philip van Dorp, Rob Ebeling, Albert G. Huizing

Radar Department
TNO Defence, Security and Safety
The Hague, The Netherlands
philip.vandorp@tno.nl

Abstract— High resolution radar imaging techniques can be used in ballistic missile defence systems to determine the type of ballistic missile during the boost phase (threat typing) and to discriminate different parts of a ballistic missile after the boost phase. The applied radar imaging technique is 2D Inverse Synthetic Aperture Radar (2D-ISAR) in which the Doppler shifts of various parts of the ballistic missile are employed to obtain a high cross-range resolution while the resolution in downrange is achieved with a large radar bandwidth. For a 10 cm downrange resolution, a radar bandwidth of more than 1.5 GHz is required. However, this requirement is not compatible with EM frequency spectrum allocations for long range ballistic missile defence radars that operate in the L, S, and C frequency band. In this paper, a novel coherent multiband ISAR imaging technique is proposed that employs two or more narrowband radar systems that operate in different frequency bands. The coherent multiband imaging process uses an advanced interpolation technique to achieve a very high downrange resolution and produces little artifacts due to noise.

I. INTRODUCTION

For an effective battle management and command & control process in ballistic missile defense systems, detailed information about the location and type of threat and the timing of events such as the separation of the warhead and the booster is crucial. Non-Cooperative Target Recognition (NCTR) techniques which estimate the geometry of the object require a high range resolution for identifying individual object scatterers for correct classification. For this purpose, phased array radars are needed that not only detect and track ballistic missiles during boost phase but also provide high resolution images of these missiles with resolutions on the order of 10 cm. 2D Inverse Synthetic Aperture Radar (2D-ISAR) is a radar imaging technique that employs the Doppler shifts of various parts of the ballistic missile to obtain a high cross-range resolution while the resolution in downrange is achieved with a large radar bandwidth. For a 10 cm downrange resolution, a radar bandwidth of at least 1.5 GHz is required. However, this bandwidth requirement is not compatible with Electro Magnetic (EM) frequency spectrum allocations for radars that operate in the L, S, and C frequency

band, as is shown in Table I. Only X-band radars are able to provide the desired range resolution.

TABLE I. MAIN RADAR FREQUENCY BANDS

Radar Band	Frequency (MHz)	Resolution (cm)
L	1215 – 1400	81
S	2700 – 3400	21
C	5250 – 5820	25
X	8500 – 10400	8
L - S	1215 – 3400	7

In 1997, Cuomo et al. described an ultra wideband (UWB) coherent processing technique that allows high resolution images of radar targets to be made using sparse frequency subband measurements [1]. This technique allows the desired range resolution of 10 cm to be achieved by using measurements in the L-band and S-band which are compatible with frequency spectrum allocations and long range radar operations, see Table I. To obtain the desired resolution with sparse frequency subband measurements, Cuomo et al. use a model fitting and parameter estimation technique to interpolate between the measured target frequency data. However, this procedure is sensitive to noise and leads to artifacts in the radar image. In this paper, a different approach is described in which cross-range imaging is performed first and then the interpolation of the downrange measurements is performed. This approach is less sensitive to noise and produces less artifacts in the high resolution radar image.

The paper is organized as follows. Section II gives an overview of the ISAR imaging technique. Section III discusses coherent multiband processing. Section IV shows bandwidth interpolation applied on real measurements and ISAR simulation results and section V draws conclusions.

II. ISAR IMAGING

High range resolution radars transmit waveforms which are designed to optimize the range resolution. This is achieved by transmitting pulses with frequency and/or phase modulation. One of these waveforms is the Linear Frequency

Modulated (LFM) pulse with bandwidth B . On receive, stretch processing can be used to obtain a range profile of a target with a high range resolution. Details of stretch processing are provided by Tait [2], Schikorr [3] and Blanton [6]. The stretch processing measurements is a sinusoidal output signal where the frequency is proportional to the range and range processing with Fourier transform is applied. The similarities between stretch processing radars and processing for linear Frequency Modulated Continuous Wave (FMCW) radars mean that the proposed approach is applicable to both radar types.

In the next subsections the ISAR processing is introduced followed by the ISAR accuracies.

A. ISAR processing

Wide band radar scattering from a target is often used to form an image of the target. The image is a synthetic aperture radar image (SAR image) or an inverse synthetic aperture radar image (ISAR image) because the transformation behaves as if a very large aperture radar antenna is synthesized from a set of incremental data taken over the domain of the (synthetic) aperture. The SAR image is formed by moving the radar system while the target remains stationary, and the ISAR image is formed by holding the radar at a fixed location while the orientation angle of the target changes. The image transformation involves first transforming the time domain data to the range domain using a spectral estimation usually based on a Fourier transform. Then the complex cross-range data for each range value is transformed to the Doppler domain using another spectral estimation, also usually a Fourier transformation. For a rotating target, some points on the target are moving toward the radar (positive Doppler) and some are moving away (negative Doppler). The down range and cross range data are combined and give the image domain of the target.

There are many implementations of the SAR/ISAR concept. Some use the two independent Fourier transformations as described (possibly in reverse order), while others use a 2-D version of the Fourier transform. If the increments are (or can be made) uniform and equal (often including a transformation to Cartesian frequency then the fast Fourier Transform (FFT) can be used. Fig. 1 presents the ISAR processing architecture. The digitized measurements enter the architecture in the top left corner. M sweeps (first index) are stored with N samples (second index) in the linear sweep. The architecture presents two routes which are reversible with linear transformations.

- The blue route (clock wise) weights each sweep with a range window and succeed with the range FFT. This step gives the range response. The cross-range processing selects one range cell (column), weights each range response with a cross-range window, and succeeds with the cross-range FFT. The result is the ISAR response.
- The green route (anti clock wise) selects one received frequency (column), weights each frequency response with a cross-range window and succeeds with the cross-range FFT. This processing step gives the cross-

range response. The range processing weights each cross-range response with a range window, and succeeds with the range FFT. The result is the ISAR response.

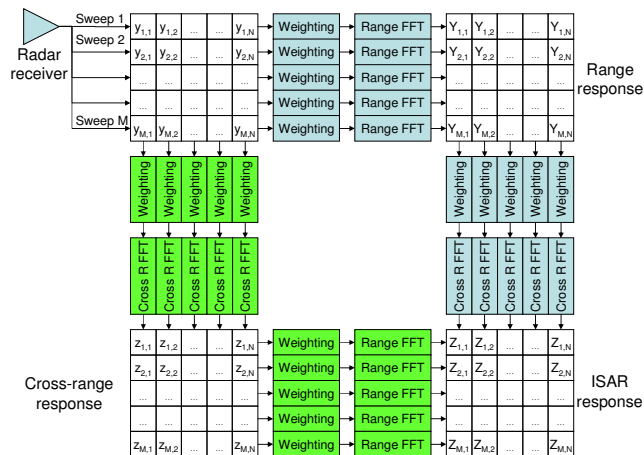


Figure 1. ISAR processing architecture.

B. ISAR Processing with Bandwidth Interpolation

Irregular motion of the object disturbs phase of the measurements and range migration gives unaligned range responses. Compensation techniques are applied which reduce the effects of these disturbances on the ISAR image. The quality of the ISAR image is very sensitive for these compensation techniques. Normally, the phase correction is applied before the range processing and the range alignment is applied after the range processing.

The bandwidth interpolation applied to measurements of different radar bands extends the bandwidth. The resulting bandwidth comprises all the other bands and gives a high range resolution ISAR image. The bandwidth interpolation introduces errors which disturb the ISAR image. There are two possible approaches for bandwidth interpolation in the ISAR imaging process. The first approach is to perform bandwidth interpolation before range processing and cross-range processing (the clockwise approach). The Fourier transforms are linear processes and the bandwidth interpolation errors add twice. The second approach is to perform bandwidth interpolation before the cross-range processing (the anti-clockwise approach). The bandwidth interpolation errors add only once in the cross-range processing. These approaches are now described in more detail.

Cuomo [1] presents a HRR processing approach with bandwidth interpolation applied on the range response. His approach with additional cross-range processing is presented in Fig 2. The LFM pulses of each band are digitized. The measurements are the input of the bandwidth interpolation (BWI). The output of BWI is a signal which contains the individual bands and interpolated signals in the gaps between

the bands. The processing continues with range processing, range alignment and cross-range processing.

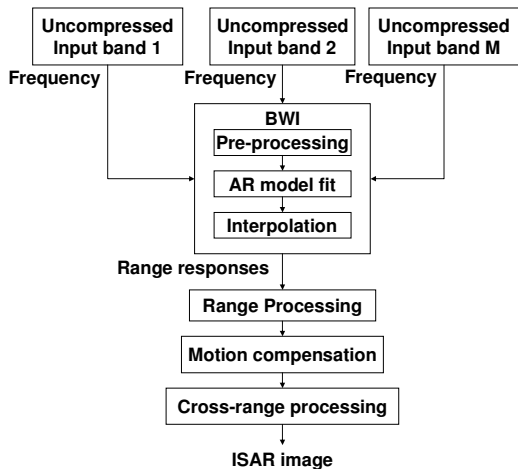


Figure 2. ISAR processing approach with range BWI before cross-range processing.

In this paper, we propose a different approach to minimize the bandwidth interpolation errors, see Fig 3. The phase correction and range alignment are applied onto each band individually before cross-range processing. The range alignment is a complex multiplication in the frequency domain. The cross-range processing is applied on each band and results in cross-range responses of each individual band. The cross-range responses contain no bandwidth interpolation errors and gives optimal cross-range object separation. The bandwidth interpolation is applied onto each cross-range response. This process generates errors in range not in the cross-range response. The final step is the range processing applied onto each interpolated cross-range response.

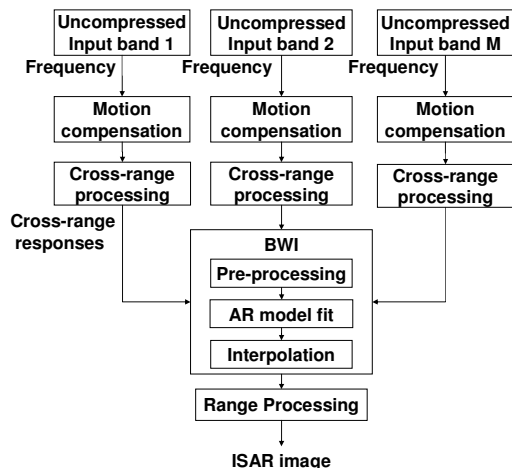


Figure 3. ISAR processing approach with range BWI after cross-range processing.

C. ISAR Accuracies

The linear sweep FMCW range resolution Δr is related with the bandwidth B of the transmitted sweep [2]:

$$\Delta r = w_{range} \frac{c}{2B} \quad (1)$$

where c is the speed of light and w_{range} a window correction factor. It follows from this equation that a better range resolution can be achieved by increasing the bandwidth. The window function is applied to reduce strong sidelobes which mask weak signals from other objects. A rectangular shaped window has $w = 1$ with -13.2 dB sidelobes, a Hamming window has $w = 1.3$ with -40 dB sidelobes. The cross-range resolution Δr_{cross} given by the change in aspect angle $\Delta\psi$ of the target during the M sweeps of one ISAR image [2]:

$$\Delta r_{cross} = w_{cross} \frac{\lambda}{2\Delta\psi} \quad (2)$$

where λ is the average transmitter frequency wavelength and w_{cross} a window correction factor. The reason of the cross-range window and range window are equivalent. The cross-range resolution is independent of the range but depends on the target motion. Correction of the cross-range is possible with the target track.

The ISAR imaging is induced by changes in the aspect angle of the target. During the imaging time, the scatterers must remain in their range cells. Reflectivity density function won't remain the same over a wide range of radar viewing angles. Therefore we cannot use an arbitrary large integration time to achieve the highest possible cross-range resolution and prevent defocusing in the image.

III. COHERENT MULTIBAND PROCESSING

This section describes the pre-processing, AR model fit and interpolation techniques of coherent multiband processing.

A. Pre-Processing

Different radar bands cause systems errors which depend on the radar circuits. Common system errors are offsets, unequal power and phase alignment. These systems errors are removed before the ISAR processing.

The radar measurements have multiple bands. The frequency spacing of the bands differs and the grids have no common factors. The analysis is more complicated than that of regularly sampled data. We resample the irregularly measurements onto a regular grid with the Fourier transform. By computing the Fourier coefficients at all required discrete frequencies and then Fourier-transforming back, a kind of interpolation can be obtained.

B. AR model fit

Kauppinen [4] presents a good overview of signal extrapolation without a detailed description of the Burg method. Roth and Keiler [5] give a good description of the Burg's method applied onto one band. The Burg method estimates a model in a recursive manner with reduced computational effort. We adapt this for our problem.

First, we describe the single band AR filter estimation and multiband AR filter estimation.

1) Single Band AR Filter Estimation

The auto-regressive (AR) model is defined by the equation:

$$y_n = -\sum_{m=1}^{m=P} a_m y_{n-m} + e_n \quad (3)$$

where y_n are the signal samples, P is the model order, a_m are the model coefficients, and e_n is the residual. The model coefficients a_m are calculated by minimizing the total energy of the residual:

$$E = \sum_{all\ n} |e_n|^2 \quad (4)$$

The Burg method is one method to solve this problem and described by Roth [5]. The errors in the forward and backward directions are:

$$e_n = \sum_{m=1}^P a_m y_{n-m} + y_n = \sum_{m=0}^P a_m y_{n-m} \quad (5)$$

where $a_1 = 1$. This FIR filter is implemented with a lattice filter structure. The equations of the lattice filter are:

$$f_n^l = f_n^{n-1} + k_l b_{n-1}^{l-1} \quad (6)$$

$$b_n^l = b_n^{n-1} + k_l^* f_{n-1}^{l-1} \quad (7)$$

Where f_n^l and b_n^l are the forward and backward prediction errors and k_l are the reflection coefficients of the l stage. The $*$ denotes the complex conjugate operation. The initial values for the residuals are $f_n^0 = b_n^0 = y_n$. Burg's method calculates the reflection coefficients k_l so that they minimize the sum of the forward and backward residual error. This implies an assumption that the AR coefficients can predict the signal forward and backward. The sum of the residual error in the l -th stage is:

$$E_l = \sum_{n=l}^{N-1} w_n |f_n^l|^2 + w_n |b_n^l|^2 \quad (8)$$

Minimizing E_l with respect to the reflection coefficient k_l yields $\partial E_l / \partial k_l = 0$. The reflection coefficient that full fills the partial derivative is given by:

$$k_l = \frac{-2 \sum_{n=l}^{N-1} (w_n f_n^{l-1}) b_{n-1}^{l-1*}}{\sum_{n=l}^{N-1} (w_n f_n^{l-1}) f_n^{l-1*} + (w_n b_{n-1}^{l-1}) b_{n-1}^{l-1*}} \quad (9)$$

The AR coefficients a_m can be obtained from the reflection coefficients k_l via the Levinson-Durbin algorithm. The recursion is initialized with $a_0^0 = 1$ and

$$a_m^l = a_m^{l-1} + k_l a_{l-m}^{l-1*} \text{ for } m = 1, 2, \dots, l-1 \quad (10)$$

$$a_l^l = k_l \quad (11)$$

This process is repeated for $l = 1, 2, \dots, P$. At the end of the iterations a_m^P gives the desired prediction error filter coefficients a_m of the AR filter.

2) Multi-band AR filter estimation

The multiple band approach has M bands. The measurements are indicated with f_j and b_j each with N_j elements where j is the band index. The Burg method has M datasets which are related to each other. The FIR filter is applied on each of the M chirps. The sum of the residual error in the l stage is the sum of all forward measurements error and the sum of all backward measurements error. The combined error function is:

$$E_l = \sum_{j=1}^M \sum_{n=l}^{N-1} w_{j,n} |f_{j,n}^l|^2 + w_{j,n} |b_{j,n}^l|^2 \quad (12)$$

The solution of the partial derivative is:

$$k_l = \frac{-2 \sum_{j=1}^M \sum_{n=l}^{N-1} (w_{j,n} f_{j,n}^{l-1}) b_{j,n-1}^{l-1*}}{\sum_{j=1}^M \sum_{n=l}^{N-1} (w_{j,n} f_{j,n}^{l-1}) f_{j,n}^{l-1*} + (w_{j,n} b_{j,n-1}^{l-1}) b_{j,n-1}^{l-1*}} \quad (13)$$

The a update is equivalent with the single band approach applied to each band:

$$f_{j,n}^l = f_{j,n}^{n-1} + k_l b_{j,n-1}^{l-1} \quad (14)$$

$$b_{j,n}^l = b_{j,n}^{n-1} + k_l^* f_{j,n-1}^{l-1} \quad (15)$$

The results of the combined Burg estimation is one FIR filter applicable on all bands.

C. Interpolation and Extrapolation

Band-width interpolation is an extension to extrapolation. Assume that the forward extrapolated signal in a missing band is y_n^f and the backward extrapolated signal is y_n^b . The missing band is a weighted sum of both extrapolated signals:

$$y_n = w_n y_n^f + (1 - w_n) y_n^b, \quad (16)$$

where w_n is a scale factor which controls the transition between the two bands. We use a linear scale factor starting with one at the beginning of the band and zero at the end of the band. This weighting is depicted in Fig 4. The Figure shows a linear weighting in case of interpolation starting at one and zero at the end of the band. The Extrapolation has no weighting, it contains the predicted signals.

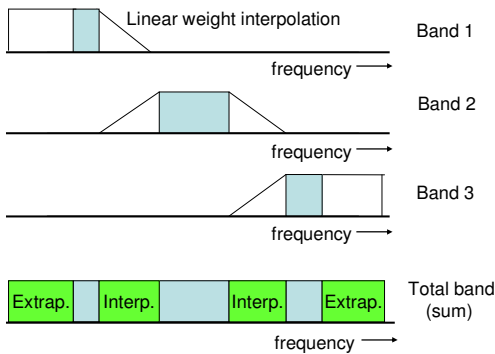


Figure 4. Bandwidth interpolation with linear weights and bandwidth extrapolation.

IV. RESULTS

Two experiments are carried out applying the described method. The first experiment contains a three corner test measurement with range processing. The second experiment contains a simulated ballistic missile trajectory with FMCW measurements succeeded with ISAR processing.

A. Test Measurements

The test measurement contains three corners with different height and positioned in the near field antenna and radar cross section (RCS) measurement facility of TNO. The FMCW frequency is 10-20 GHz with 10 MHz frequency step. The corresponding range resolution is 0.015 m. We remove 80% of the total band. The remaining lower band is 10-11 GHz and higher band is 19-20 GHz. The resolution of both bands is 0.15 m. The model order P is chosen one third of the number of measurements in the shortest band according to Roth and Keiler [5]. Fig 5 presents the results of the interpolation. The measurement contains five heights with each 40 angle measurements with a total angle deviation of approximately

30 degrees. The five height measurements show the varying ranges of the three corners as a function of the aspect angle. The middle corner is the rotation centre of the measurement.

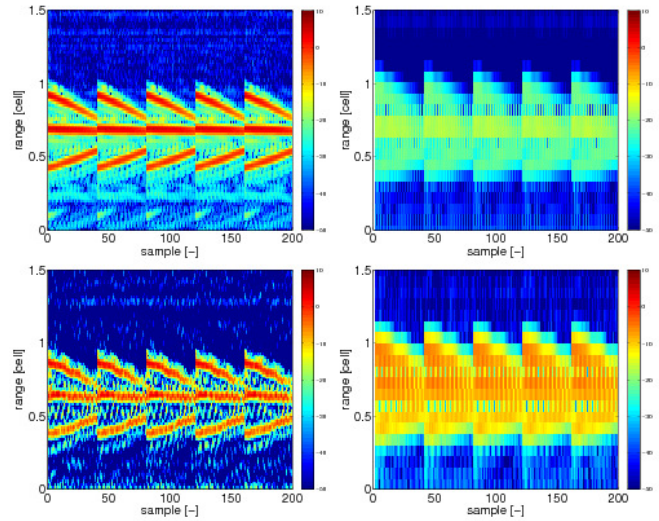


Figure 5. Interpolated three corners test measurements. Left top the original full band range measurement. Right top the lower band range measurement. Right bottom the higher band range measurement. Left bottom the interpolated range measurement.

The lower band and higher band range resolution causes indistinguishable corners which are distinguishable in the original full band. The interpolated range response shows the three corners. The interpolated range response shows besides the three corners other distortions which are also visible in the full band range measurement. The interpolated measurement shows no artifacts caused by the applied method. The selected model order is not critical. The applied Burg method converges to the correct solution regardless of the chosen number of poles. In our case the number of poles is larger than the three corners. This prevents that the number of poles has to be estimated. One of the reasons of the convergence is the minimizing of the forward and backward prediction errors of the Burg method. The recursive Burg method does not require much computation time compared with other AR estimation methods.

B. Simulated Ballistic Missile Measurements

For the simulated Ballistic Missile Measurements a software program is used which is capable of generating LFM pulse measurements. The program which is used is called RAPPORT (Radar signature Analysis and Prediction by Physical Optics and Ray Tracing) and is developed in house at TNO. It uses a combination of Geometrical Optics (GO) and Physical Optics (PO) methods to calculate the radar return of a specified object. The object is a 3D CAD model, consisting of a large number of triangular facets. RAPPORT uses GO to determine which facets of the CAD model are hit by rays from the radar's EM radiation. The PO calculating method is then used to determine the amount of reflected radiation for each facet which is hit by the radar's EM radiation. This is done for all facets and the returning radiation is summed over all facets, resulting in one amplitude and phase. This can be done for all

possible frequencies and aspect angles with respect to the object. Therefore, when a frequency sweep and a number of aspect angles are defined, ISAR measurements can be generated.

The target in this experiment is a 3D CAD representation of the ballistic missile, see Fig 6. This particular CAD model consists of 6374 facets and the length of the missile is approximately 9 meters. In this simulation we investigate the results of ISAR imaging using an L-band radar with frequency band 1.2 – 1.4 GHz and an S-band radar with a frequency of 3.0 – 3.4 GHz. The frequency step is 2.2 MHz. The gap is estimated with bandwidth interpolation as described in the previous section. After the missile launch, the radar tracked the missile along its trajectory. The missile trajectory has duration of approximately one minute. Fig 7 presents the results of one ISAR image along its track.

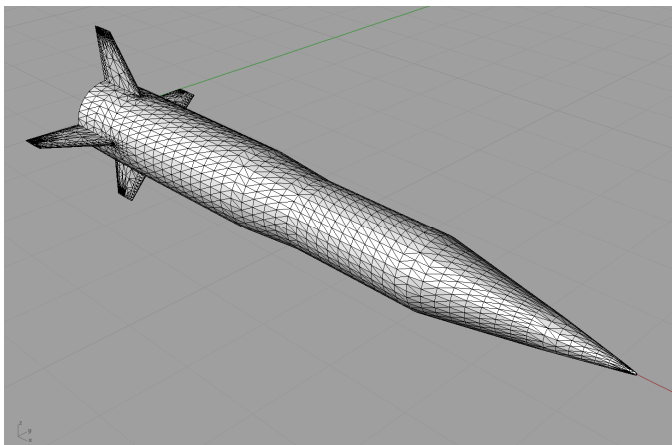


Figure 6. 3D CAD representation of a ballistic missile.

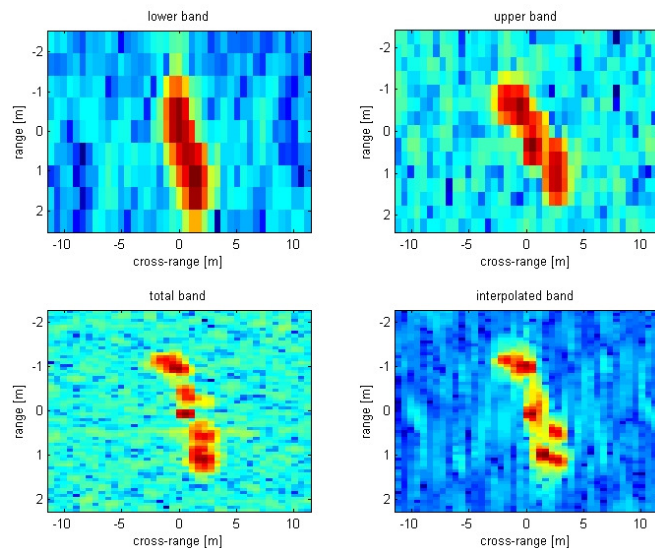


Figure 1

Figure 7. ISAR response of a multiband radar. Left top L-band radar ISAR image. Right top S-band radar ISAR image. Left bottom complete band ISAR image. Right bottom bandwidth interpolated ISAR image with L-band and S-band measurements.

The ISAR images in the Figure are generated with equivalent range grid and cross-range grid. The L-band and S-band ISAR images show less detail than the full-band and bandwidth interpolated ISAR images. The bandwidth interpolated ISAR shows the details not available in the individual bands. The bandwidth interpolation applied with first range processing followed with cross range processing has artifacts in the range direction of the ISAR image. These artifacts are not visible in our method. The applied method shows no artifacts caused by the applied method. The described method is evaluated with different signal-to-noise ratios of the missile response by adding noise to the measurements. Adding noise causes different detail available in the full band ISAR image. The bandwidth interpolated ISAR image shows an equal amount of detail compared with the full band ISAR image. The applied Burg method gives reliable results for all signal-to-noise ratios.

V. CONCLUSIONS

In this paper, a novel coherent multiband processing technique has been described that allows high resolution radar images of targets such as ballistic missiles to be made at very long ranges. The method presented in this paper is less sensitive to noise and produces less artifacts in the ISAR image than the method described by Cuomo et al. for ultra-wideband coherent processing. The applied Burg auto-regressive model estimation method is very stable, gives reliable results and is used in real-time applications.

REFERENCES

- [1] K.M. Cuomo, J.E. Piou, and J.T. Mayhan, "Ultra-Wideband Coherent Processing" The Lincoln Laboratory Journal, Volume 10, Number 2, 1997, pp. 203 - 222.
- [2] P. Tait, "Introduction to Radar Target Recognition", IEEE radar, sonar, navigations series, London, 2005
- [3] M. Schikorr, "High range resolution with digital stretch processing", Proceedings IEEE Radar Conference 2008, 26-30 May, Rome.
- [4] I. Kauppinen, J. Kauppinen, and P. Saarinen, "A method for long extrapolation of audio signals", J. Audio Eng. Soc., Vol. 49, No. 12, pp. 1167-1180, Dec. 2001.
- [5] K. Roth, I. Kauppinen, P.A.A. Esquef, and V. Välimäki, "Frequency warped Burg's method for AR-modelling", 2003 IEEE Workshop on Applications of Signal Processing to Audio and Acoustics, October 19-22-, 2003, New Paltz, NY, USA.
- [6] J.L. Balnton, "Cued medium-PRF air-to-air radar using stretch range compression" Proceedings of the 1996 IEEE National Radar Conference, 13-16 May, Ann Arbor, MI, USA.